

This document contains a post-print version of the paper

## Estimation and control of the tool center point of a mobile concrete pump

authored by **J. Henikl, W. Kemmetmüller, and A. Kugi**

and published in *Automation in Construction*.

---

The content of this post-print version is identical to the published paper but without the publisher's final layout or copy editing. Please, scroll down for the article.

---

### Cite this article as:

J. Henikl, W. Kemmetmüller, and A. Kugi, "Estimation and control of the tool center point of a mobile concrete pump", *Automation in Construction*, vol. 61, pp. 112–123, 2016. DOI: [10.1016/j.autcon.2015.10.005](https://doi.org/10.1016/j.autcon.2015.10.005)

---

### BibTex entry:

```
@ARTICLE{Henikl_2015_Automation,  
  author = {Henikl, J. and Kemmetmüller, W. and Kugi, A.},  
  title = {{E}stimation and control of the tool center point of a mobile concrete  
    pump},  
  journal = {{A}utomation in {C}onstruction},  
  year = {2016},  
  volume = {61},  
  pages = {112-123},  
  doi = {10.1016/j.autcon.2015.10.005}  
}
```

---

### Link to original paper:

<http://dx.doi.org/10.1016/j.autcon.2015.10.005>

---

### Read more ACIN papers or get this document:

<http://www.acin.tuwien.ac.at/literature>

---

### Contact:

Automation and Control Institute (ACIN)  
Vienna University of Technology  
Gusshausstrasse 27-29/E376  
1040 Vienna, Austria

Internet: [www.acin.tuwien.ac.at](http://www.acin.tuwien.ac.at)  
E-mail: [office@acin.tuwien.ac.at](mailto:office@acin.tuwien.ac.at)  
Phone: +43 1 58801 37601  
Fax: +43 1 58801 37699

---

### Copyright notice:

This is the authors' version of a work that was accepted for publication in *Automation in Construction*. Changes resulting from the publishing process, such as peer review, editing, corrections, structural formatting, and other quality control mechanisms may not be reflected in this document. Changes may have been made to this work since it was submitted for publication. A definitive version was subsequently published in J. Henikl, W. Kemmetmüller, and A. Kugi, "Estimation and control of the tool center point of a mobile concrete pump", *Automation in Construction*, vol. 61, pp. 112–123, 2016. DOI: [10.1016/j.autcon.2015.10.005](https://doi.org/10.1016/j.autcon.2015.10.005)

# Tool Center Point Position Control of a Mobile Concrete Pump<sup>★</sup>

J. Henikl<sup>a</sup>, W. Kemmetmüller<sup>a</sup>, A. Kugi<sup>a</sup>

<sup>a</sup>Automation and Control Institute, Vienna University of Technology, Vienna, Austria

## Abstract

Booms of modern mobile concrete pumps are vulnerable to elastic vibrations due to the light-weight construction. Although these vibrations can be effectively damped with appropriate controllers, the residual movement of the tool center point (TCP) during the pumping process is still uncomfortable for the workers guiding the end hose. This movement can be compensated with a simple position controller for the last joint of the boom in combination with a damping controller. The required measurement of the height of the tool center point is, however, difficult in practice. In this paper, a strategy for the determination of the height of the tool center point based on the kinematic description of the boom is proposed. For this purpose, the measurement of the inclination of each boom segment with inertial sensors in combination with an observer concept is presented which circumvents the disadvantages of tilt sensors. It is shown that a complementary filter design utilizing an additional inertial sensor placed on the tool center point allows for the practical implementation of a PD control loop which effectively compensates the vertical movement. The estimation and control concept is evaluated by means of simulation studies on a validated mathematical model of a mobile concrete pump.

*Key words:* flexible link manipulator; hydraulic actuators; concrete pump; feedback control; sensor fusion.

## 1 Introduction

The development in the construction of booms of modern mobile concrete pumps, see, e.g., Figure 1, is driven by the requirement of a reduction of the static load. A boom with less weight enables a higher operating range and the usage of trucks with a smaller number of wheel axles. However, the reduced weight yields also a reduced stiffness which makes the system vulnerable to elastic vibrations. These vibrations, which are primarily stimulated by the pumping of wet concrete and the manual control of the boom movement by the operator, complicate the operating of such systems. The vibrations due to the boom movement can be reduced by experienced operators. However, a reduction of the excitations during the pumping process is very difficult. This excitation of the system is caused by the non-homogeneous flow of the wet concrete, which cannot be avoided due to the construction of the double piston concrete pump. If the

period of the pumping cycle is near to the resonance frequency of the boom, the resulting large elastic vibrations can be dangerous for the workers at the end hose. For this reason, the development of tailored mathematical models and the design of control strategies for active vibration damping is a topic of current research.



Fig. 1. Mobile concrete pump with four joints.

<sup>★</sup> The authors gratefully acknowledge the financial support by TTControl GmbH and the Austrian Research Promotion Agency (FFG), Project No. 2426433.

*Email addresses:* henikl@acin.tuwien.ac.at (J. Henikl), kemmetmueller@acin.tuwien.ac.at (W. Kemmetmüller), kugi@acin.tuwien.ac.at (A. Kugi).

An extensive discussion of the modeling and the control of mobile concrete pumps is given in [17]. The results are validated by means of simulation studies. In [1] and [2], a decentralized control strategy with so-called virtual spring dampers is presented. The experimental results show that the elastic vibrations can be damped effectively. Furthermore, the contribution [3] deals with the modeling and the control of the boom as well as with a model for the pumping unit of a mobile concrete pump. In [7] and [8], an experimentally calibrated simulation model for a typical mobile concrete pump is presented. This simulation model is used in [9] for the validation of a passivity-based, decentralized control law for the damping of elastic vibrations. The control strategy is an extension of the results for a single rotating beam presented in [12] and [13]. A stability proof for this concept is given in [10]. Furthermore, experimental results are presented that show the effectivity of the control law.

These scientific contributions show that effective methods for the active damping of the elastic boom vibrations exist. With the application of such control strategies, the manual operation of the boom is much simplified. Furthermore, the appearance of resonance phenomena during the pumping process is avoided. However, these control strategies do not explicitly account for the movement of the tool center point (TCP) of the boom. In particular, the vertical movement of the tool center point caused by the pumping process will be only partly compensated. The residual movement is still uncomfortable for the worker guiding the end hose. In [15], a simple position controller is proposed, where the vertical TCP movement is compensated by actuating the last joint. To measure the TCP height, ultrasonic sensors, laser sensors and string potentiometers, where the free end of the cable is fixed on the belt of the worker guiding the end hose, are suggested. However, these measurement principles turned out to be not useable in practice. The string potentiometers are uncomfortable and an unobstructed space between the emitting source (ultrasonic or laser) and the reflecting reference level could not be guaranteed. Thus, none of the proposed systems reached acceptance on the market. Up to now, no practicable direct measurement principle for the determination of the TCP height exists. One possible solution to the TCP height estimation would be an extended Kalman filter, which is based on the dynamic model of the system. Due to the large variety of boom types and the high modeling effort, this is not reasonable for practical application. Furthermore, the disturbance forces due to the concrete pumping are commonly unknown and very difficult to estimate.

In this paper, a concept for the measurement of the TCP height is presented, which is used to realize a position control loop with a simple PD controller at the last joint of the boom. This control strategy is added to the active damping strategy proposed in [9] and [10]. The estimation of the TCP height is based on a kinematic model

of the boom, using IMUs (2 axial acceleration sensor, 1 axial angular rate sensor) at each boom segment. Furthermore, an extended sensor configuration is considered, which applies an additional acceleration sensor to the TCP. The measurements of these sensors are fused by means of observers and complementary filters, see also the extensive literature on sensor fusion in attitude estimation tasks [4,5,14,16,19].

The quality of the proposed estimation strategy is analyzed by means of experimental results of a mobile concrete pump. The overall control strategy, comprising the damping and the position controller, is validated using simulation studies of a validated model.

This paper is organized as follows: In Section 2, the derivation of the mathematical model of the considered mobile concrete pump is briefly summarized. Since the proposed control strategy strongly relies on an actively damped boom, the most important issues concerning the utilized damping controllers are given in Section 3. The PD controller, the rigid body simplification, the observer and the complementary filter design are presented in Section 4. In Section 5, simulation results of a validated model are shown that demonstrate the effectivity of the proposed strategy. Finally, a short conclusion and an outlook are given in Section 6.

## 2 Dynamic model

For the analysis, the design and the verification of control strategies, a simulation model of the mobile concrete pump has been developed. For the sake of completeness, the model derived in [8,7] is summarized in the sequel.

### 2.1 Modeling of the mechanical subsystem

The following assumptions and simplifications are made for the mathematical model of the boom.

- The boom is considered as a planar manipulator.
- The truck's movement due to the dynamic load of the boom is neglected.
- The boom segments are modeled as Euler-Bernoulli beams.
- The pumping of the concrete is considered as a disturbance acting on the system.

In Figure 2, a planar flexible manipulator with  $N = 4$  beams and the corresponding hydraulic actuators is illustrated. The degrees-of-freedom are the rigid-body angles  $\varphi_i$  and the transversal deflections  $w_i(x_i)$  of the beams for  $i = 1, \dots, N$ . The overall motion of the system is described with respect to the inertial frame  $0_0x_0y_0$ . Each beam is equipped with a local coordinate frame  $0_ix_iy_i$ , where the angle  $\varphi_i$  describes the rigid-body motion of the  $i$ -th beam relative to the beam  $i - 1$ . The

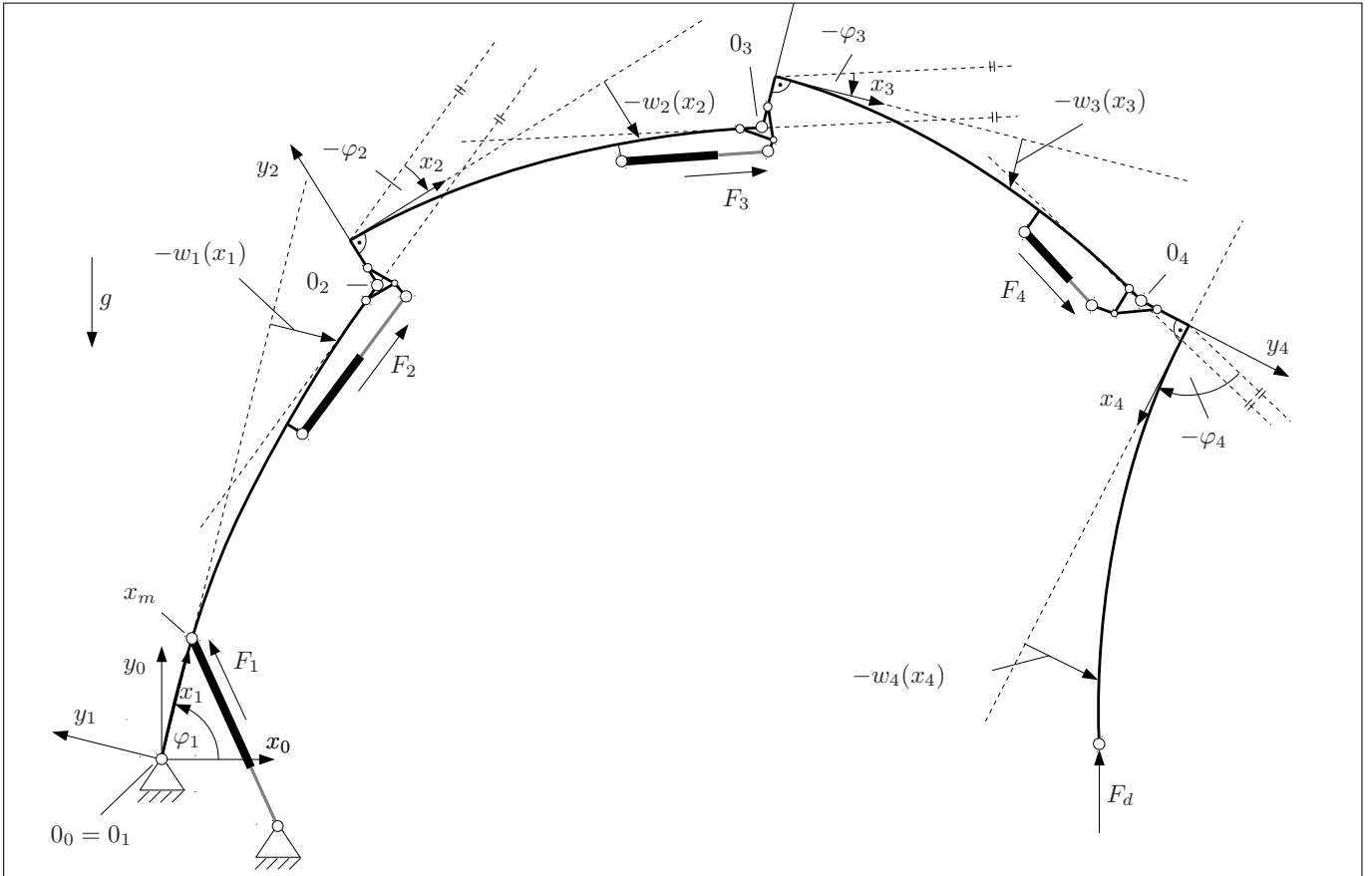


Fig. 2. Flexible manipulator with hydraulic actuation.

boom segments exhibit a bend at their beginning for  $i \geq 2$ . For this reason, the  $x_i$ -axes do not cross the joints for  $i \geq 2$ . This geometry, which is typical for mobile concrete pumps, is considered by the distances  $D_i$ , which are defined by the normal distance between the  $x_i$  axes and the tangential at the end of the bending line of the previous beam  $i - 1$ . By means of a suitable choice of the orientation of the local coordinate frames, the cylinder piston position can be described as a function of the respective rigid-body angle  $\varphi_i$  only. With this, the geometric boundary conditions for the beam deflections are given by

$$w_1(0) = 0, \quad (1a)$$

$$w_1(x_m) = 0 \quad (1b)$$

for the first joint<sup>1</sup> and

<sup>1</sup> The boundary conditions of the first boom segment differ due to the different assembling of the first hydraulic cylinder at  $x_1 = x_m$ , see Figure 2.

$$w_i(0) = 0, \quad (2a)$$

$$\left. \frac{\partial w_i(x_i)}{\partial x_i} \right|_{x_i=0} = 0 \quad (2b)$$

for  $i = 2, \dots, N$ .

The kinetic and potential energy of the system are the basis for the derivation of the mathematical model. For this, the positions and the velocities of each mass particle are described in the inertial frame  $0_0x_0y_0$ . The kinematic relations between the local and the inertial coordinate frames are given by rotation matrices and translation vectors. This transformation can be calculated in a straightforward way, see, e.g., [6], [18] and more specific for the considered mobile concrete pump, [7] and [8]. The inertial coordinates of a mass particle of the  $i$ -th beam located at  $\mathbf{r}_i^i(x_i) = [x_i, w_i(x_i)]^T$ , described in the  $i$ -th local coordinate frame (subscript), can be calculated by

$$\mathbf{r}_0^i(x_i) = \mathbf{R}_0^i \mathbf{r}_i^i(x_i) + \mathbf{d}_0^i. \quad (3)$$

The rotation matrix  $\mathbf{R}_0^i = \mathbf{R}_0^1 \mathbf{R}_1^2 \dots \mathbf{R}_{i-1}^i$ , with

$$\mathbf{R}_0^1 = \begin{bmatrix} \cos(\varphi_1) & -\sin(\varphi_1) \\ \sin(\varphi_1) & \cos(\varphi_1) \end{bmatrix} \quad (4)$$

and

$$\mathbf{R}_j^{j+1} = \begin{bmatrix} 1 & -w_j'(L_j) \\ w_j'(L_j) & 1 \end{bmatrix} \begin{bmatrix} \cos(\varphi_{j+1}) & -\sin(\varphi_{j+1}) \\ \sin(\varphi_{j+1}) & \cos(\varphi_{j+1}) \end{bmatrix} \quad (5)$$

for  $j = 1, \dots, N-1$ , describes the rotation of the local coordinate frame  $0_i x_i y_i$  with respect to the inertial frame  $0_0 x_0 y_0$ . The length of the corresponding beam is denoted by  $L_j$ . Similar to [6] small deflections and thus

$$\arctan \left( \left. \frac{\partial w_i}{\partial x_i} \right|_{x_i=L_i} \right) \approx \left. \frac{\partial w_i}{\partial x_i} \right|_{x_i=L_i} = w_i'(L_i) \quad (6)$$

are presumed. The displacement  $\mathbf{d}_0^i$  between the local coordinate frame  $0_i x_i y_i$  and the inertial frame  $0_0 x_0 y_0$  reads as

$$\mathbf{d}_0^i = \mathbf{R}_0^{i-1} \mathbf{d}_{i-1}^i + \mathbf{d}_0^{i-1}, \quad (7)$$

with  $\mathbf{d}_0^1 = [0, 0]^T$  and

$$\mathbf{d}_{j-1}^j = \mathbf{R}_{j-1}^j \begin{bmatrix} 0 \\ D_j \end{bmatrix} + \begin{bmatrix} L_{j-1} \\ 0 \end{bmatrix} \quad (8)$$

for  $j = 2, \dots, N$ .

Based on these kinematic relations and the Euler-Bernoulli assumptions, the kinetic and the potential energy of the system can be calculated. To account for non-conservative damping forces, viscous damping of the beams is included by means of the Rayleigh dissipation function. Due to the distributed-parameter character of the beams, the mathematical model of the system is given by a set of partial differential equations. To obtain a finite-dimensional approximation, henceforth the Ritz method is employed. For this purpose, a polynomial approximation  $\eta_i^b(x_i)$  of the static bending profile due to gravity of each beam is taken as the first basis function. Orthogonal polynomials  $\eta_i^o(x_i)$  are used as second basis functions [8], [7]. The approximated elastic beam deflections are defined by a superposition of the introduced basis functions

$$w_i(x_i, t) = h_i^b(t) \eta_i^b(x_i) + h_i^o(t) \eta_i^o(x_i), \quad (9)$$

for  $i = 1, \dots, N$ , with the time-varying variables  $h_i^b(t)$  and  $h_i^o(t)$ . The overall degrees-of-freedom of the mathematical model, composed of the rigid-body angles  $\varphi_i$

and the elastic degrees of freedom  $h_i^b$  and  $h_i^o$ , are combined in the vector

$$\mathbf{q} = [\varphi_1, \dots, \varphi_N, h_1^b, \dots, h_N^b, h_1^o, \dots, h_N^o]^T. \quad (10)$$

The cylinder forces  $F_i$  of the hydraulic part serve as inputs to the mechanical system. Due to the special choice of the local coordinate frames  $0_i x_i y_i$ , the cylinder piston positions  $s_{p,i}$  only depend on the rigid-body angles  $\varphi_i$ ,

$$s_{p,i} = f_i(\varphi_i), \quad (11)$$

for  $i = 1, \dots, N$ , and the vector of the generalized forces  $\mathbf{Q}_z$  describing the dynamic interconnection of the hydraulic system with the mechanical system can be calculated by means of d'Alembert's principle in the form

$$\mathbf{Q}_z^T = \left[ F_1 \frac{\partial f_1(\varphi_1)}{\partial \varphi_1}, \dots, F_N \frac{\partial f_N(\varphi_N)}{\partial \varphi_N}, 0, \dots, 0, 0, \dots, 0 \right]. \quad (12)$$

The functions  $f_i(\varphi_i)$  are defined by the geometry of the joint construction. To analyze the influence of external disturbances on the behavior of closed-loop systems (e.g., the pumping of wet concrete), a disturbing force  $F_d$  acting on the tool center point in vertical direction is considered in the model. The usage of d'Alembert's principle yields

$$\mathbf{Q}_d^T = [0, F_d] \frac{\partial \mathbf{r}_0^N(L_N)}{\partial \mathbf{q}}. \quad (13)$$

The application of the Euler-Lagrange equations

$$\frac{d}{dt} \frac{\partial T}{\partial \dot{\mathbf{q}}} - \frac{\partial T}{\partial \mathbf{q}} + \frac{\partial V}{\partial \mathbf{q}} + \frac{\partial R}{\partial \dot{\mathbf{q}}} = \mathbf{Q}_z^T + \mathbf{Q}_d^T \quad (14)$$

finally yields the simulation model of the mechanical part of the system. The resulting equations of motion can be written in the form

$$\mathbf{M}(\mathbf{q}) \ddot{\mathbf{q}} + \mathbf{c}(\mathbf{q}, \dot{\mathbf{q}}) + \mathbf{D} \dot{\mathbf{q}} + \mathbf{g}(\mathbf{q}) = \mathbf{Q}, \quad (15)$$

with the positive definite inertia matrix  $\mathbf{M}(\mathbf{q})$ , the vector of Coriolis and centrifugal forces  $\mathbf{c}(\mathbf{q}, \dot{\mathbf{q}})$ , the damping matrix  $\mathbf{D}$  and the vector of forces  $\mathbf{g}(\mathbf{q})$  related to the potential energy.

## 2.2 Modeling of the hydraulic subsystem

To fulfill the increased dynamic requirements for the application of advanced control strategies, the considered mobile concrete pump comprises a modified hydraulic architecture with control valves directly mounted at the hydraulic cylinders. For a detailed discussion of this hydraulic system the reader is referred to [9]. The dynamic

behavior of the hydraulic actuators is defined by the dynamics of the hydraulic cylinders and the proportional directional control valves. The differential equations for the chamber pressures  $p_1$  and  $p_2$  take the form

$$\dot{p}_1 = \frac{\beta}{V_{01} + A_1 s_p} (-A_1 v_p + q_1), \quad (16a)$$

$$\dot{p}_2 = \frac{\beta}{V_{02} - A_2 s_p} (A_2 v_p - q_2), \quad (16b)$$

with the bulk modulus of oil  $\beta$ , the piston areas  $A_1$  and  $A_2$ , the offset volumes  $V_{01}$  and  $V_{02}$  and the velocity  $v_p = \dot{s}_p$ . The volume flows  $q_1$  and  $q_2$  are determined by the valve position  $s_v$  and the pressure difference,

$$q_1 = \begin{cases} \alpha \sqrt{\frac{2}{\rho}} A_{v1}(s_v) \sqrt{p_s - p_1} & s_v \geq 0 \\ \alpha \sqrt{\frac{2}{\rho}} A_{v1}(s_v) \sqrt{p_1 - p_t} & s_v < 0, \end{cases} \quad (17a)$$

$$q_2 = \begin{cases} \alpha \sqrt{\frac{2}{\rho}} A_{v2}(s_v) \sqrt{p_2 - p_t} & s_v \geq 0 \\ \alpha \sqrt{\frac{2}{\rho}} A_{v2}(s_v) \sqrt{p_s - p_2} & s_v < 0, \end{cases} \quad (17b)$$

where  $\alpha$  denotes the contraction coefficient,  $\rho$  the oil density,  $p_s$  the supply pressure,  $p_t$  the tank pressure and  $A_{v1}(s_v)$  and  $A_{v2}(s_v)$  are the opening areas of the valve to chamber 1 and 2, respectively. The resulting cylinder force  $F$  acting on the mechanical part of the system can be calculated by

$$F = p_1 A_1 - p_2 A_2 - F_R(v_p), \quad (18)$$

where the first part accounts for the pressure force generated by the cylinder and  $F_R(v_p)$  summarizes the friction forces of the cylinder.

### 3 Active damping control

In this section, the control strategy for the active damping of the elastic vibrations of the boom is described. The motivation, derivation and proof of stability of the presented passivity-based control law is presented in [9] and [10]. The basis of the control law is the assumption that the angular velocities  $\dot{\varphi}_n$  can be assumed as virtual control inputs to the system. This can be achieved by means of the so-called servo compensation applied to the hydraulic actuators, which compensates their non-linear behavior, and the assumption that the rigid body dynamics in combination with the hydraulic system is much faster than the dynamics of the elastic boom movement. This assumption is feasible for the considered mobile concrete pump, see [9].

It can be shown by the analysis of the time derivative of the total energy of a planar manipulator with an arbitrary number  $N$  of serially linked Euler-Bernoulli beams

as given in Figure 2 that the local feedback of the dynamic part of the beam deflection at the boundaries  $x_i = 0$  for  $i = 1, \dots, N$  renders the system dissipative if the joint angular velocities can be assumed as control inputs.<sup>2</sup> Thus, the joint angular velocities and the beam deflections represent the collocated pairings of the system, cf. [10].

However, the feedback of the beam deflections alone does not lead to an asymptotically stable behavior of the overall system. For this purpose, the addition of a position controller for each joint is necessary. The control law used for the active damping of the considered system is then given by

$$u_i^c = k_{1,i} \left. \frac{\partial^2 w_i(x_i)}{\partial x_i^2} \right|_{x_i=0} - k_{2,i} (\varphi_i - \varphi_i^d), \quad (19)$$

with the desired joint angle  $\varphi_i^d$  and the controller parameters  $k_{1,i}, k_{2,i}$ . The damping injection is proportional to the coefficients  $k_{1,i}$ , while higher values of  $k_{2,i}$  cause a faster decay of position errors. It is shown in [10] that the application of (19) with arbitrary coefficients  $k_{1,i}, k_{2,i} > 0$  leads to an asymptotically stable overall system in any configuration of the related rigid body angles if the underlying velocity controllers are ideal.

The application of the control strategy to the considered mobile concrete pump is discussed in the following: The beam deflections and the joint angles are measured by strain gauges and inclination sensors. Due to gravity, the stationary beam deflection is in general different from zero and has to be subtracted from the measurement signal previous to feeding it to the damping controller. The calculation of this stationary beam deflection is, however, not accurate due to the limited model accuracy. Therefore, high-pass filters are used instead for the extraction of the dynamic part of the signal. Figure 3 illustrates the implementation of the control strategy for a single boom segment with the index  $i$ . The system is represented by the boom and the hydraulic actor HA<sub>*i*</sub>. The beam deflection, given by the strain gauge signal  $\varepsilon_{SG,i}$ , is filtered by a high-pass filter HP<sub>*i*</sub>. The control input  $u_i = u_i^d + u_i^c$  consists of the part  $u_i^d$  desired by the operator or a higher ranked control system and the feedback part  $u_i^c$  according to (19). The corresponding valve position  $s_{v,i}$  is obtained from the servo compensation SC<sub>*i*</sub>.

### 4 PD control of the tool center point

Simulation studies show that the remaining movement of the tool center point (after applying the damping controller of the previous section) can be compensated effectively with an additional PD position controller for the

<sup>2</sup> Note that the beam deflections are proportional to the respective joint torques.

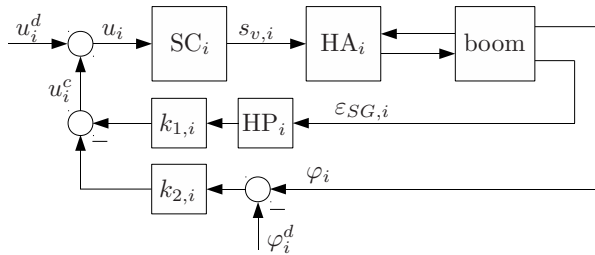


Fig. 3. Control structure for the  $i$ -th beam.

last joint of the boom. The simulations are based on the model developed in [7] and [8]. In Figure 4, the simulated vertical movement of the tool center point  $y_T = r_{0,y}^4(L_4)$  (which is the  $y_0$  coordinate of the vector  $\mathbf{r}_0^4(L_4)$ ) during a periodic excitation of the boom by a vertical acting force  $F_d$  at the tool center point is illustrated.

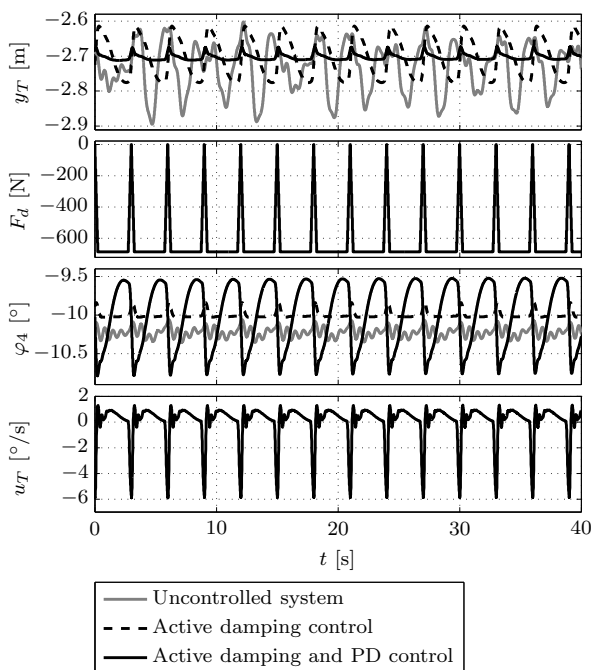


Fig. 4. PD control assuming ideal measurement of the TCP height.

In this scenario, the quasi steady-state behavior (all transient processes due to the beginning of the pumping process are decayed) of the boom (i) without any feedback control, (ii) with active damping control and (iii) the combination of active damping and PD control is compared. The shape, the period and the amplitude of the disturbance force  $F_d$  is chosen such that the pumping process is qualitatively approximated, see, e.g., [3,11]. The reason for the special shape is the discontinuous transition between the cycles of the concrete pump. The amplitude of 700 N relates to the weight of the wet concrete fitting in the end hose. The chosen cycle time

of 0.3 Hz is typical for real pumping units. The chosen joint angles  $\varphi_1 = 10^\circ$  and  $\varphi_2 = \varphi_3 = \varphi_4 = -10^\circ$  represents a sprawled boom configuration, which is pose with a relatively low rigidity, see Figure 5.

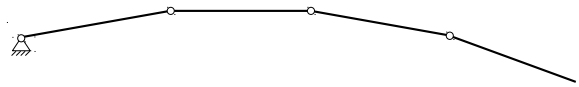


Fig. 5. Boom configuration pumping scenario.

Figure 4 shows that with active damping control the movement of the tool center point is considerably reduced. However, the residual movement cannot be compensated with the damping control alone and is still uncomfortable for the worker guiding the end hose. However, assuming that  $y_T$  can be measured, the movement can be further reduced to a few cm with an additional PD controller of the form

$$R_{PD}(s) = k_{T,P} + k_{T,D} \frac{s}{1 + sT_R}, \quad (20)$$

with the Laplace variable  $s$  and  $U_T(s) = R_{PD}(s)Y_T(s)$  with the Laplace transforms  $Y_T(s)$  and  $U_T(s)$  of the measured output  $y_T$  and the control input  $u_T$  (the desired angular velocity of the last joint), respectively. The control input  $u_T$  and the resulting movement of the last joint are also illustrated in Figure 4. The coefficients  $k_{T,P}$  and  $k_{T,D}$  have been tuned by means of the Ziegler-Nichols method and the time constant  $T_R$  is chosen to reduce the influence of measurement noise.

In practice, the desired value for the height of the tool center point is defined by the operator in the idle state (no pumping of concrete). Since the exact amount and weight of wet concrete in the pipes is unknown, an accurate calculation of the idle state is not possible. Thus, instead of controlling the height directly, only the variations are minimized. Therefore, a high-pass filter

$$G_{HP}(s) = \frac{s}{s + \omega_{HP}} \quad (21)$$

with the cutoff frequency  $\omega_{HP}$  chosen to  $\omega_{HP} = 1 \text{ s}^{-1}$  is proposed for the extraction of control error. A possible drift of the height of the tool center point due to the high pass filter is avoided by the position controller of the active damping control, see (19). The resulting structure of the control loop for the considered system is illustrated in 6.

The simulation results in Fig. 4 show that the vertical movement of the tool center point can be significantly reduced with this relatively simple position controller. For this purpose, however, the measurement of the TCP height is necessary.

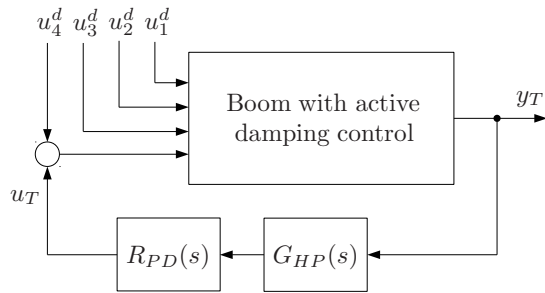


Fig. 6. PD control loop assuming ideal measurement of the TCP height.

#### 4.1 Measurement of the TCP height

As discussed in the introduction, no measurement principle for the direct determination of the TCP height (i.e. the ground distance) is known, which meets the requirements of the practical application. Therefore, the aim is to estimate the height, if possible by means of the available sensor configuration only.

The height of the tool center point depends on the joint angles and the elastic deformation of the boom segments. The kinematic description of the system can be approximately simplified to a rigid body problem if the inclinations in the middle of the boom segments are measured. This can be motivated by taking a look at Figure 7, which illustrates two deformed boom segments with the

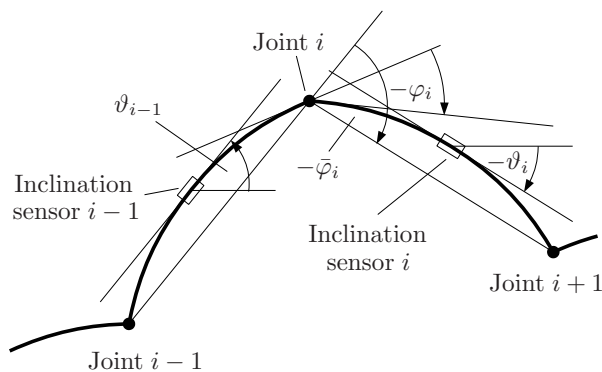


Fig. 7. Rigid body approximation with inclination measurement.

indices  $i$  and  $i - 1$  of a planar, flexible manipulator. The joint angles are again denoted by  $\varphi_i$ . According to the mean value theorem there exists at least one point on the bending line of each boom segment, where the tangent

of the bending line is parallel to the straight line, which connects the neighboring joints  $i - 1$  and  $i$ . If the profile of the bending line is approximated by a circular arc, this point is exactly in the middle of the boom segment. Thus, the difference of the measured inclinations  $\vartheta_i$  and  $\vartheta_{i-1}$  of sensors mounted at these points corresponds to the enclosed angle  $\bar{\varphi}_i$  of the straight lines between the joints,  $\bar{\varphi}_i = \vartheta_i - \vartheta_{i-1}$ . Under the additional assumption of small beam deflections, the distance between the joints is given by the length of the corresponding boom segment. With these prerequisites, the coordinates of the tool center points in the inertial frame can be described in the form

$$\bar{\mathbf{r}}_0^N(L_N) = \bar{\mathbf{R}}_0^N \bar{\mathbf{r}}_N^N(L_N) + \bar{\mathbf{d}}_0^N, \quad (22)$$

using a similar notation as in Section 2. The vector  $\bar{\mathbf{r}}_N^N(x_N) = [x_N, 0]^T$  denotes the coordinates of a point on the  $x_N$ -axis, defined in the local coordinate frame  $0_N x_N y_N$ . The rotation of the local coordinate frame  $0_N x_N y_N$  with respect to the inertial frame  $0_0 x_0 y_0$  is given by  $\bar{\mathbf{R}}_0^N = \bar{\mathbf{R}}_0^1 \bar{\mathbf{R}}_1^2 \dots \bar{\mathbf{R}}_{N-1}^N$  with

$$\bar{\mathbf{R}}_{i-1}^i = \begin{bmatrix} \cos(\bar{\varphi}_i) & -\sin(\bar{\varphi}_i) \\ \sin(\bar{\varphi}_i) & \cos(\bar{\varphi}_i) \end{bmatrix} \quad (23)$$

for  $i = 1, \dots, N$ . The displacement  $\bar{\mathbf{d}}_0^i$  between the local coordinate frame  $0_i x_i y_i$  and the inertial frame  $0_0 x_0 y_0$  reads as

$$\bar{\mathbf{d}}_0^i = \bar{\mathbf{R}}_0^{i-1} \bar{\mathbf{d}}_{i-1}^i + \bar{\mathbf{d}}_0^{i-1}, \quad (24)$$

with  $\bar{\mathbf{d}}_0^1 = [0, 0]^T$  and  $\bar{\mathbf{d}}_j^{j+1} = [L_j, 0]^T$  for  $j = 1, \dots, N$ . Alternatively, a formulation of (22) can be found which directly uses the measured inclinations  $\vartheta_i$ . The height of the tool center point  $y_T$  is then determined by the  $y_0$ -coordinate of the vector  $\bar{\mathbf{r}}_0^N(L_N)$ .

The drawback of this approach is that an accurate measurement of the inclinations  $\vartheta_i$  is difficult, especially in dynamic movements. Sensors available on the market, are typically composed of accelerometers with two orthogonal axes designed in MEMS technology. Any translational acceleration of these sensors results in a measurement error since the movement cannot be distinguished from the change of the orientation in the gravitational field. In particular, elastic vibrations of the boom during the pumping process lead to the measurements of partly highly increased amplitudes of the inclination signal, which do not coincide with the real movement. In Figure 8, the already described pumping scenario with activated damping control is shown. Here, the calculated height of the tool center point is compared to the rigid body approximation using once a perfect inclination sensor and once a realistic inclination sensor. This realistic sensor model includes a 2-axial acceleration sensor with

a low pass filter<sup>3</sup> with a cutoff frequency of 5 Hz for the suppression of high frequency signals. It can be seen that the rigid body approximation with perfectly assumed measurements fits the simulated height of the tool center point very well. Contrary, the using of realistic inclination sensors causes large errors. Thus, the direct application of the described PD control-loop according to (6) is not possible with this type of measurement.

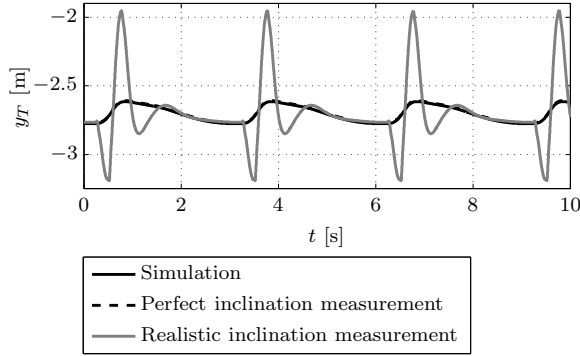


Fig. 8. Measurement of TCP with ideal and realistic inclination sensors.

#### 4.2 Observer for inclination estimation with inertial sensor

To compensate the systematic measurement error occurring in classical inclinations sensors, the usage of inertial sensors which include a gyroscope in addition to the 2-axial acceleration is typically proposed. The gyroscope measures the angular rate of the inclination which is not influenced by translational movements. Integration of the angular velocity with respect to time yields the inclination. This integration is, however, afflicted with errors due to the bias typically occurring in gyroscopes. Thus, the idea is to combine the measurement of the acceleration sensors, which give good results for static or slow scenarios, with the gyroscope measurements, which are accurate for fast scenarios. Different approaches for the fusion of these sensor signals can e.g. be found in [4,5,14,16,19].

If the acceleration sensor is oriented such that the plane spanned by the two measurement axes  $\xi_I$  and  $\zeta_I$  is parallel to the gravitational vector  $\mathbf{g}$ , the inclination determined by the acceleration sensor can be calculated by, cf. Figure 9,

$$\vartheta_a = \text{atan}(-a_\xi, -a_\zeta). \quad (25)$$

<sup>3</sup> Sensors available on the market typically comprise manually tunable filters for the suppression of vibrations, see, e.g., <http://www.sensor-technik.de> or <http://www.gemachemnitz.de>.

The two measured accelerations are denoted by  $a_\xi$  and  $a_\zeta$ . The measurement  $\vartheta_a$  coincides with the real inclination  $\vartheta$  in static situations. To account for the systematic measurement error in dynamic situations, the disturbance model  $\vartheta_a = \vartheta + d_a$ , with the zero mean disturbance  $d_a$ , is defined.

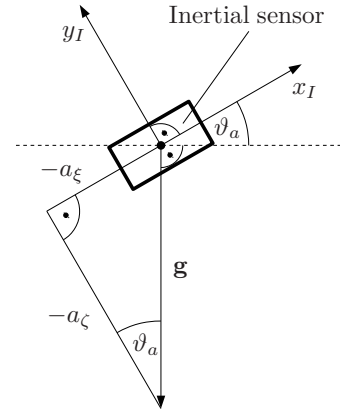


Fig. 9. Geometry for the measurements of the inertial sensor.

The dynamics of the gyroscope measurement is modeled by

$$\dot{\vartheta} = \omega_g - b_g, \quad (26a)$$

$$\dot{b}_g = 0, \quad (26b)$$

with the measured angular velocity  $\omega_g$  and the bias, see, e.g., [4,5,14]. Numerous methods are reported in literature which discuss the combination of these sensors signals to accurately estimate the attitude of rigid body objects. Typically, extended Kalman filters [14,16], uncented Kalman filters [4] or complementary filters [19] are proposed, where the multiplicative extended Kalman filter implementation is probably used in most applications, see, e.g. [5] for an excellent overview.

In this work, the system is linear which significantly simplifies the design. In the first step, a time discrete Luenberger observer in the form

$$\hat{\vartheta}_{k+1} = \hat{\vartheta}_k - T_a \hat{b}_{g,k} + T_a \omega_{g,k} + \hat{k}_\vartheta (\hat{\vartheta}_k - \vartheta_{a,k}), \quad (27a)$$

$$\hat{b}_{g,k+1} = \hat{b}_{g,k} + \hat{k}_b (\hat{\vartheta}_k - \vartheta_{a,k}), \quad (27b)$$

is designed, with the sample time  $T_a$ , the measured inclination  $\vartheta_{a,k}$  of the accelerometers (25), the measured angular velocity  $\omega_{g,k}$  of the gyroscope, the estimated values  $\hat{\vartheta}_k$  and  $\hat{b}_{g,k}$ , and the observer gains  $\hat{k}_\vartheta$  and  $\hat{k}_b$ . Intro-

ducing the observer error

$$\mathbf{e}_k = \begin{bmatrix} \hat{\vartheta}_k - \vartheta_k \\ \hat{b}_{g,k} - b_{g,k} \end{bmatrix}, \quad (28)$$

and  $\vartheta_{a,k} = \vartheta_k + d_{a,k}$ , the error dynamics is given by

$$\mathbf{e}_{k+1} = \underbrace{\begin{bmatrix} 1 + \hat{k}_\vartheta & -T_a \\ \hat{k}_b & 1 \end{bmatrix}}_{\Phi_e} \mathbf{e}_k - \underbrace{\begin{bmatrix} \hat{k}_\vartheta \\ \hat{k}_b \end{bmatrix}}_{\Gamma_d} d_{a,k}. \quad (29)$$

The eigenvalues of the dynamic matrix  $\Phi_e$  can be adjusted by means of the observer gains. Moreover, the influence of translational accelerations can be reduced by using small values for the observer gains. This, however, has the drawback that errors resulting from the bias of the gyroscope increase. Thus, a compromise between these two criteria has to be found based on the movements typically occurring in the considered application.

The observer strategy has been implemented and tested at the industrial mobile concrete pump presented in [8,9,7,10]. For this purpose, all four boom segments have been equipped with an inertial sensor of the type NGS1 of SENSOR-TECHNIK WIEDEMANN.<sup>4</sup> This sensor type measures the accelerations and angular velocities in all three orthogonal axes and possesses the protection class IP67 according to the IEC standard 60529 required for off-highway machines. The same observer gains with the values  $\hat{k}_\vartheta = -5 \times 10^{-3}$  and  $\hat{k}_b = 1 \times 10^{-4} \text{ s}^{-1}$  have been chosen for the observers of the individual segments of the boom. This parameterization has been found to be useful during the experimental investigations. In Figure 10, the measurement results of the inclination of the fourth boom segment are shown. The inclination, determined by the observer is compared to the inclination measured by the acceleration sensors only. Furthermore, the respective measured accelerations and angular velocity are illustrated. It can be seen that the estimation of the observer signal has a significantly reduced signal noise. With classical inclination sensors, a noise reduction is only possible by the use of low pass filters which can be problematic for closed-loop control. The essential benefit of the proposed observer design is, however, the suppression of the measurement errors due to translational accelerations. In particular, peaks of the measurement signal at abrupt velocity changes can be seen in Figure 10 which do not correspond to the real boom movement. These errors are compensated effectively by the proposed observer.

The observer strategy has also been integrated in the simulation model with the experimentally tested observer gains. Figure 11 shows the simulated true inclina-

<sup>4</sup> <http://www.sensor-technik.de>

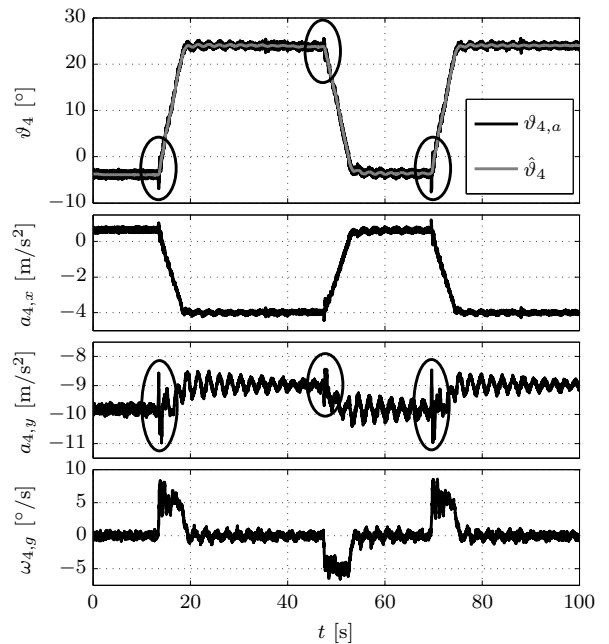


Fig. 10. Experimental validation of the observer design.

tions  $\vartheta_i$ , the inclinations measured only by the acceleration sensors  $\vartheta_{i,a}$  and the inclinations determined by the observers  $\hat{\vartheta}_i$  for  $i = 1, \dots, 4$  at the previously described pumping scenario. Thereby, the behavior of the system with activated damping control without PD control of the tool center point is considered. The estimated signals fit the real values very good for the first three boom segments  $i = 1, \dots, 3$ . At the fourth boom segments, however, increased deviations can be seen.

Taking a look at the corresponding height  $y_T$  of the TCP, see Figure 12, it can be seen that already a rather accurate estimation can be obtained by the proposed observer. The estimation errors, especially in the fourth boom segment, however, still lead to a considerable estimation error of approximately 5 cm for dynamic movements of the system. Thus, it can be assumed that the control performance of the PD-control strategy presented at the beginning of this section in combination with the observer will still not completely fulfill the demands of the real application.

#### 4.3 Complementary filter design

To improve the estimation accuracy especially for fast movements of the boom, an additional inertial sensor for the acceleration is placed at the tool center point. Given an estimation of the inclination, the vertical part of the acceleration can be determined. Twice integration of this vertical part yields a measurement signal, which covers fast dynamic movements very accurately. This measurement is, however, meaningless for slow movements and

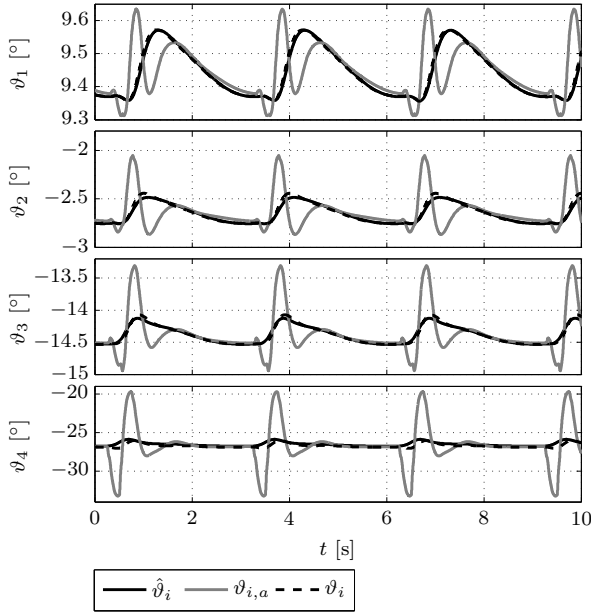


Fig. 11. Simulation results of the proposed observer for the 4 boom segments.

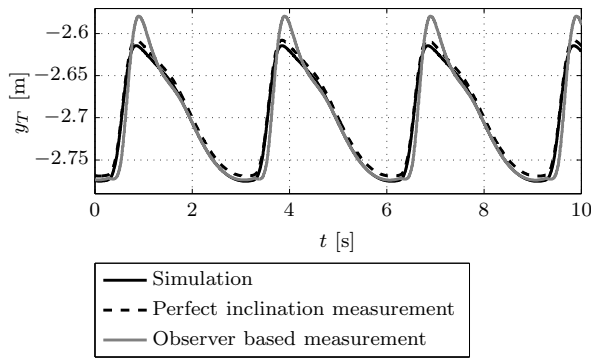


Fig. 12. Comparison of estimation results of the observer based measurement with the ideally assumed inclination measurements.

static scenarios, since double integration yields fast increasing accumulated errors. In this case, fortunately, the estimation of the height by means of the observed inclinations and the kinematics (22) of the system gives very good results. Thus, the advantages of both estimation strategies are combined by complementary filters. For this purpose, the height  $\hat{y}_{T,\vartheta}$  obtained by the inclinations is filtered by a low pass with an appropriate cut-off frequency whereas the twice integrated acceleration signal  $a_{T,y}$  is filtered by a complementary high pass with the same cutoff frequency. In this work two complemen-

tary filters of the form

$$G_{CF,\vartheta}(s) = \frac{\omega_{CF}}{s + \omega_{CF}}, \quad (30a)$$

$$G_{CF,a}(s) = \frac{s}{s + \omega_{CF}} \quad (30b)$$

with the cutoff frequency  $\omega_{CF}$  are utilized. To avoid a drift of the estimated TCP height, the twice integration of the measured acceleration requires filtering with an additional high pass

$$G_{HP,a}(s) = \frac{s}{s + \omega_a} \quad (31)$$

with a lower cutoff frequency  $\omega_a < \omega_{CF}$ . The acceleration of the tool center point is measured by a 2-axial acceleration sensor. To obtain the vertical part  $\hat{a}_{T,y}$ , the acceleration signals  $a_{T,\xi}$  and  $a_{T,\zeta}$ , and the estimated inclination  $\hat{\vartheta}_T$  of the proposed observer are combined with

$$\hat{a}_{T,y} = a_{T,\xi} \sin(\hat{\vartheta}_T) + a_{T,\zeta} \cos(\hat{\vartheta}_T). \quad (32)$$

The combined estimated TCP height then reads as

$$\hat{Y}_T(s) = G_{CF,\vartheta}(s)\hat{Y}_{T,\vartheta}(s) + \frac{G_{HP,a}(s)G_{CF,a}(s)}{s^2}\hat{A}_{T,y}(s). \quad (33)$$

Thereby,  $\hat{A}_{T,y}(s)$ ,  $\hat{Y}_{T,\vartheta}(s)$  and  $\hat{Y}_T(s)$  denote the Laplace transforms of  $\hat{a}_{T,y}$ ,  $\hat{y}_{T,\vartheta}$  and the combined measurement result  $\hat{y}_T$ . In Figure 13, a block diagram summarizes the complementary filter design.

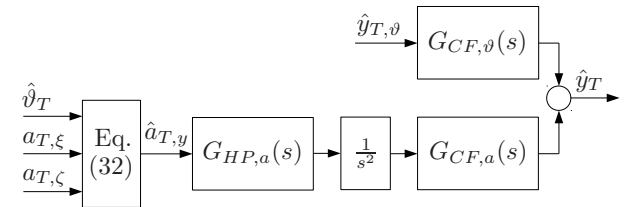


Fig. 13. Complementary filter design.

Figure 14 shows the simulated pumping scenario with the complementary filter design in comparison to the results with the observer design only. In this simulation, the filter is parameterized with the cutoff frequencies  $\omega_{CF} = 0.5 \text{ s}^{-1}$  and  $\omega_a = 0.2 \text{ s}^{-1}$ . It can be seen that the deviations of the estimation at the acceleration peaks due to the pumping discontinuations are compensated very good.

Since the beam deflection of the fourth boom segment has a minor influence on the TCP height in comparison

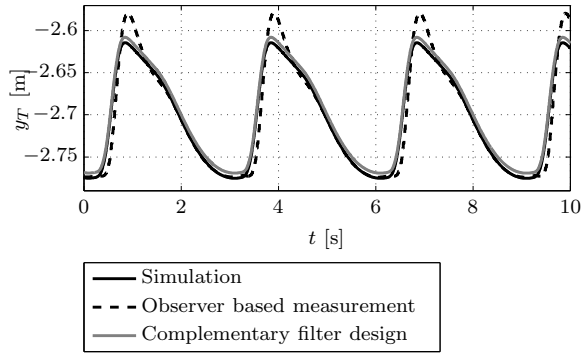


Fig. 14. Comparison of estimation results of the observer based measurement without and with the additional complementary filter design.

to the boom segments 1 to 3, the inertial sensor at the fourth boom segment could be attached directly on the tool center point. Then, no additional sensor would be necessary and the number of sensors is identical to the original version.

### 5 Simulation results

This section discusses simulation results of the PD control strategy with active damping control and complementary filter based estimation of the TCP height. In Figure 15, the uncontrolled system, the system with active damping control and the system with active damping and PD control are compared for a typical pumping scenario.

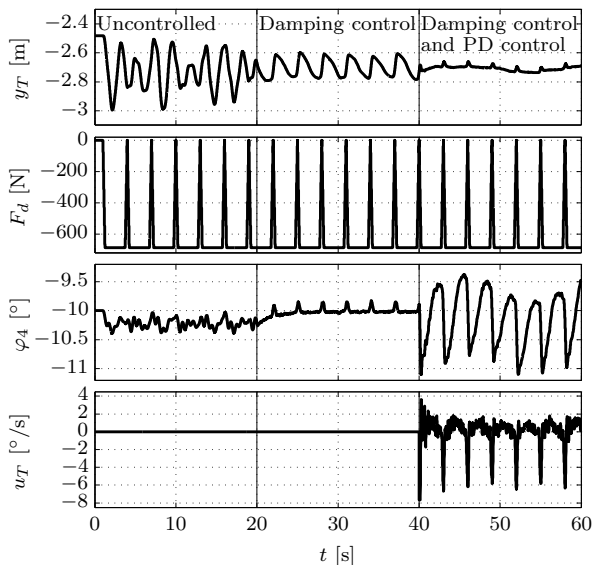


Fig. 15. Comparison of the uncontrolled system, the system with active damping control and the system with active damping and PD control with realistic sensor properties.

The different control strategies are activated at the times  $t = 20$  s and  $t = 40$  s. Furthermore, the disturbing influence of measurement noise and typical bias values of the acceleration sensors and gyroscopes is considered. The respective parameters were adjusted according to the signal quality of the inertial sensors used for the mobile concrete pump. It can be seen that the movements due to the concrete pumping can be effectively reduced similar to the results with an ideal measurement of the TCP height. Moreover, the performance of the control loop is not significantly deteriorated by the realistic sensor properties.

To prove that the proposed control strategy yields also good results at different boom configurations, a second pumping scenario with the working points of the joint angles given by  $\varphi_1 = 60^\circ$ ,  $\varphi_2 = -60^\circ$ ,  $\varphi_3 = -45^\circ$  and  $\varphi_4 = 45^\circ$ , see Figure 16, has been simulated. In this

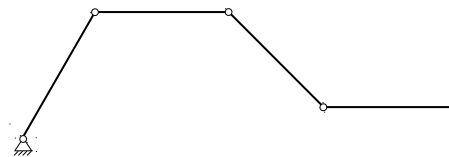


Fig. 16. Second boom configuration pumping scenario.

configuration the boom is significantly stiffer than the boom configuration considered before. As it is proven in Figure 17, the vertical movement of the tool center point is also reduced to only a few cm in this scenario. It has to be noted that the same parameters of the control and estimation strategy as in the first configuration have been used.

### 6 Conclusions and outlook

The results of this work show that the vertical movement of the tool center point due to a cyclic excitation like the pumping process can be effectively reduced to a few cm with the proposed control and estimation strategy. Hence, there is a huge potential for the improvement of the conditions for the workers guiding the end hose. However, one essential point still has to be clarified for the real application of the algorithms: The coefficients of the PD controller were manually tuned according to the considered pumping scenario. Due to the nonlinearity of the system, the adaption of the coefficients depending on the configuration of the boom is required since the movement of the last joint has a different influence on the TCP height at different inclinations of the last boom segment. Furthermore, the TCP height can not be manipulated by the last joint if the last segment is aligned vertically. In order to compensate the vertical movements at these boom configurations, the control strategy has to be extended to the use of further joints of the boom. For this purpose, the extension of the algorithms for the determination of the participating joints

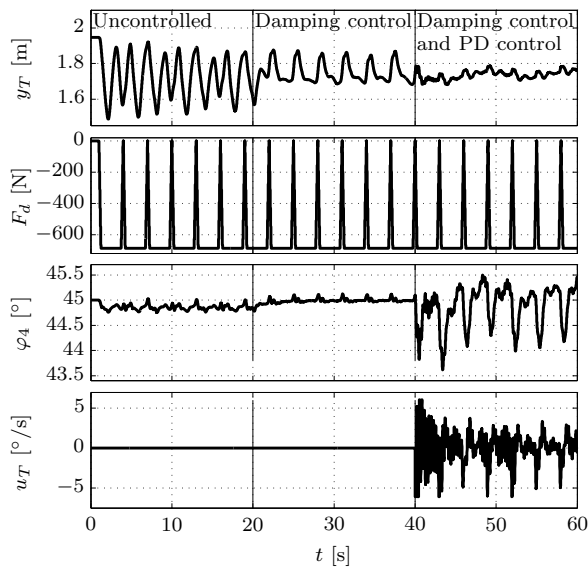


Fig. 17. Comparison of the uncontrolled system, the system with active damping control and the system with active damping and PD control with realistic sensor properties at a second boom configuration.

and for the adjustment of the controller parameters are topic of current research.

## References

- [1] W. Bernzen. On vibration damping of hydraulically driven flexible robots. In *Proc. of the 5th IFAC Symposium on Robot Control*, pages 677–682, Nantes, France, 1997.
- [2] W. Bernzen, D. Nissing, and H. Schwarz. On vibration control of a concrete pump. In *Proc. of the European Control Conference*, Karlsruhe, Germany, 1999.
- [3] G. Cazzulani, C. Ghielmetti, H. Giberti, F. Resta, and F. Ripamonti. A test rig and numerical model for investigating truck mounted concrete pumps. *Automation in construction*, 20:1133–1142, 2011.
- [4] J. L. Crassidis and F. L. Markley. Unscented filtering for spacecraft attitude estimation. *Journal of Guidance, Control, and Dynamics*, 26(4):536–542, 2003.
- [5] J. L. Crassidis, F. L. Markley, and Y. Cheng. Survey of Nonlinear Attitude Estimation Methods. *Journal of Guidance, Control, and Dynamics*, 30(1):12–28, 2007.
- [6] A. De Luca and B. Siciliano. Closed-Form Dynamic Model of Planar Multilink Lightweight Robots. *IEEE Trans. on Systems, Man and Cybernetics*, 21(4):826–839, 1991.
- [7] J. Henikl, W. Kemmetmüller, M. Bader, and A. Kugi. Modelling, simulation and identification of a mobile concrete pump. *Mathematical and Computer Modelling of Dynamical Systems*, 99(9):999–999, 2014.
- [8] J. Henikl, W. Kemmetmüller, and A. Kugi. Modeling and Simulation of Large-Scale Manipulators with Hydraulic Actuation. In *Proc. of the 7th Vienna Conference on Mathematical Modeling*, pages 780–785, Vienna, Austria, 2012.
- [9] J. Henikl, W. Kemmetmüller, and A. Kugi. Modeling and Control of a Mobile Concrete Pump. In *Proc. of the 6th IFAC Symposium of Mechatronic Systems*, pages 91–98, Hangzhou, China, 2013.
- [10] J. Henikl, W. Kemmetmüller, T. Meurer, and A. Kugi. Infinite-Dimensional Decentralized Damping Control of Large-Scale Manipulators with Hydraulic Actuation. *Automatica*, submitted May 2014.
- [11] H. Liu, W. Li, and Q. Zhao. Measuring Method of Concrete Pump Discharge Based on Pressure. In *Proc. of the IEEE International Conference on Robotics and Biomimetics*, pages 1527–1531, Bangkok, Thailand, 2008.
- [12] Z. H. Luo. Direct Strain Feedback Control of Flexible Robot Arms: New Theoretical and Experimental Results. *IEEE Trans. on Automatic Control*, 38(11):1610–1622, 1993.
- [13] Z. H. Luo, B. Z. Guo, and O. Morgül. *Stability and Stabilization of Infinite Dimensional Systems with Applications*. Springer-Verlag, London, UK, 1999.
- [14] F. L. Markley. Attitude error representations for kalman filtering. *Journal of Guidance, Control, and Dynamics*, 26(2):311–317, 2003.
- [15] Putzmeister-Werk Maschinenfabrik GmbH. Mobile concrete pumping unit with segmented delivery arm. Patent application, Germany, Nr. DE19503895A1; Inventor: K. Schlecht; Priority date: 07.02.1995; Published: 08.08.1996.
- [16] S. I. Roumeliotis, G. Sukhatme, and G. A. Bekey. Smoother based 3D attitude estimation for mobile robot localization. In *Proc. of the IEEE International Conference on Robotics and Automation*, volume 3, pages 1979–1986, Detroit, US, 1999.
- [17] M. Schneider. *Modellbildung, Simulation und nichtlineare Regelung elastischer, hydraulisch angetriebener Großraummanipulatoren*. VDI Fortschrittsberichte Reihe 8., VDI Verlag, Düsseldorf, Germany, 1999.
- [18] A. A. Shabana. *Dynamics of Multibody Systems*. Cambridge University Press, New York, US, 2005.
- [19] A. Tayebi, S. McGilvray, A. Roberts, and M. Moallem. Attitude estimation and stabilization of a rigid body using low-cost sensors. In *Proc. of the 46th IEEE International Conference on Decision and Control*, volume 3, pages 6424–6429, New Orleans, US, 2007.